

Effect of vanadium and titanium modification on the microstructure and mechanical properties of a microalloyed HSLA steel

B.K. Show¹, R. Veerababu*, R. Balamuralikrishnan, G. Malakondaiah

Defence Metallurgical Research Laboratory, Kanchanbagh P.O., Hyderabad 500058, Andhra Pradesh, India

ARTICLE INFO

Article history:

Received 22 July 2009

Received in revised form 16 October 2009

Accepted 22 October 2009

Keywords:

HSLA steel

Plates

TEM

Precipitates

ThermoCalc

ABSTRACT

DMR-249A is a low carbon microalloyed high-strength low-alloy (HSLA) steel. While DMR-249A plates of thickness less than 18 mm meet the specified room temperature yield strength (390 MPa) and Charpy impact toughness (78J at -60°C) in the as-rolled condition, thicker plates require water quenching and tempering. Elimination of the quenching and tempering treatment can result in significant cost and energy savings besides offering increased productivity. Therefore, in the present work, modifications to the base DMR-249A steel composition have been investigated with the objective of producing thicker gage plates (24 mm) capable of meeting the specified properties in the normalized condition. Plates from three modified compositions i.e., containing 0.015 wt.% titanium and 0.06, 0.09 and 0.12 wt.% vanadium respectively and one composition with 0.10 wt.% vanadium, and without any titanium were investigated over a range of normalizing temperatures (875–1000 $^{\circ}\text{C}$). In all cases, only the steel without titanium met the specified properties in the normalized condition. Microstructural investigations using scanning and transmission electron microscopy, as well as support evidence from calculations performed using ThermoCalc software, suggest that this is due to the presence of nanoscale vanadium rich carbonitride particles distributed throughout the matrix. These particles were absent in the titanium-containing steel at a similar vanadium level.

© 2009 Elsevier B.V. All rights reserved.

1. Introduction

Microalloyed high-strength low-alloy (HSLA) steels are essentially low carbon low-alloy steels that contain small additions (0.001–0.1 wt.%) of alloying elements such as Nb, V, or Ti [1]. These steels exhibit an outstanding combination of high strength, resistance to brittle fracture and good weldability, particularly if the carbon content is kept below ~ 0.1 wt.% [2–4]. Several categories of HSLA steels have been developed catering to the needs of specific applications, such as the construction of large ships, oil and gas transmission lines, and offshore oil drilling platforms [2,4,5].

DMR-249A is a low carbon (0.08 wt.% C) HSLA steel, of nominal composition (in wt.%) 1.5 Mn, 0.75 Ni and 0.2 Si, with micro-alloying additions of 0.03–0.05 V, <0.05 Nb and 0.01–0.06 Ti. The steel is designed to have a predominantly ferritic microstructure, with pearlite less than 10% by volume. Large size plates of this steel are required for shipbuilding applications [6], in thicknesses ranging

from 3.15 to 40 mm, and must meet stringent mechanical property specifications (Table 1). Typically, plates of lower thickness are able to meet the specified properties in the as-rolled or normalized condition, but heavier gage (>18 mm) plates require a water quenching and tempering (WQ+T) treatment in order to meet both strength and toughness requirements consistently [6]. The objective of the work reported here was to improvise upon the DMR-249A composition to examine whether the required combination of strength and sub-zero impact toughness can be achieved in the normalized condition for heavier gage plates. The main motivation was to achieve significant cost and energy savings as well as increase the productivity by eliminating the need for WQ+T treatment. In other words, the goal of the composition modification was to produce a material which, in the normalized condition, will have yield strength greater than the base material by about 50–60 MPa and with CVN impact energy greater than ~ 100 J at -60°C , for a plate thickness of 24 mm.

Significant amount of literature exists on the production of normalized grades of microalloyed HSLA steel [7,8]. These steels are typically normalized 30–50 $^{\circ}\text{C}$ above the Ac_3 temperature. The actual normalizing temperature should be chosen such that it allows for complete re-austenitization of microstructure but also does not permit extensive austenite grain growth, as the average ferrite grain size in the product is significantly influenced by the grain size of the parent austenite. It is to be noted that the original

* Corresponding author at: Electron Microscopy Group, Defence Metallurgical Research Laboratory, Kanchanbagh P.O., Hyderabad 500058, Andhra Pradesh, India. Tel.: +91 4024586729; fax: +91 40 24343587.

E-mail addresses: bijay_show@rediffmail.com (B.K. Show), veeru_met@yahoo.com (R. Veerababu), bmk_pgh@yahoo.com (R. Balamuralikrishnan), director@dmrl.drdo.in (G. Malakondaiah).

¹ Presently at: National Institute of Technology, Durgapur, West Bengal, India.

Table 2
Mechanical properties of the experimental steels in the as-rolled condition.

Steel	YS ^a (MPa)	UTS ^a (MPa)	Elongation (%)	Impact toughness, J ^{a,b}
A	417	593	26.0	6, 4, 4 (5)
B	475	620	17.0	3, 4, 4 (4)
C	445	610	26.3	5, 4, 4 (4)
D	455	600	28.0	5, 5, 4 (5)

^a For each steel, the reported values are average of minimum two (for tensile properties); for impact toughness all values are listed with average in brackets.

^b Charpy V-notch test at -60°C .

subsequently twin jet electropolished with mixed acids (by volume: 78% methanol, 10% lactic acid, 7% sulfuric acid, 3% nitric acid and 2% hydrofluoric acid) electrolyte at -30°C . The thin foils were examined in a FEI Tecnai 20T transmission electron microscope operated at 200 kV and equipped with an EDAX EDS system.

3. Results

3.1. Mechanical properties

As-rolled plates from all the steels satisfactorily meet the tensile requirements, but exhibit rather poor impact toughness at -60°C (Table 2). The mechanical property data in the normalized condition (Table 3; Fig. 2) shows that on the average plates from all steels under the different normalizing conditions meet the impact toughness specifications, but only samples from steel D and the steel A sample normalized at 975°C meet the yield strength requirement. Amongst other samples, while the ones from steels A and B normalized at 950°C fall just short of the yield strength specification of 390 MPa, the rest have yield strengths in the range of 310–370 MPa (Table 3). It is evident that only steel D reliably meets both strength and impact toughness requirements in the normalized condition. It is significant that there is no titanium present in steel D while the other three steels contain ~ 0.015 wt.% titanium.

The following observations can be made with respect to the mechanical properties of the normalized samples:

- (a) On the average, for any given steel, YS increases with increase in normalizing temperature, while the sub-zero CVN impact energy decreases with increasing normalizing temperature. It has also been observed that the scatter in CVN/impact energy increases with increasing normalizing temperature (Fig. 2b).

Table 3
Mechanical properties of the experimental steels in the normalized condition.

Steel	Normalizing ^a temperature ($^{\circ}\text{C}$)	YS ^b (MPa)	UTS ^b (MPa)	Elongation ^b (%)	Impact toughness, J ^{b,c}
A	875	370	520	33.4	222, 298, 298 (273)
	900	361	512	33.5	
	925	357	527	35.0	173, 196, 253 (207)
	950	389	546	33.9	168, 188, 206 (187)
	975	395	555	27.3	24, 121, 194 (113)
B	875	330	503	28.0	206, 298, 298 (267)
	900	357	523	32.0	247, 298, 298 (281)
	950	389	544	33.1	224, 241, 299 (255)
C	875	310	540	35.5	299, 299 (299)
	900	368	554	27.3	
D	875	396	525	34.0	278, 280, 286 (281)
	900	418	537	34.0	184, 244, 280 (236)
	925	411	538	27.6	184, 184, 188 (185)
	950	413	559	28.2	124, 189, 202, 277, 298 (218)
	975	442	581	27.6	12, 146, 174, 199, 200 (146)
	1000	445	595	25.8	72, 171, 191 (145)

^a Austenitized at temperature for 1h followed by air-cooling to room temperature.

^b For each steel, the reported values are average of minimum two (for tensile properties); for impact toughness all values are listed with average in brackets.

^c Charpy V-notch test at -60°C .

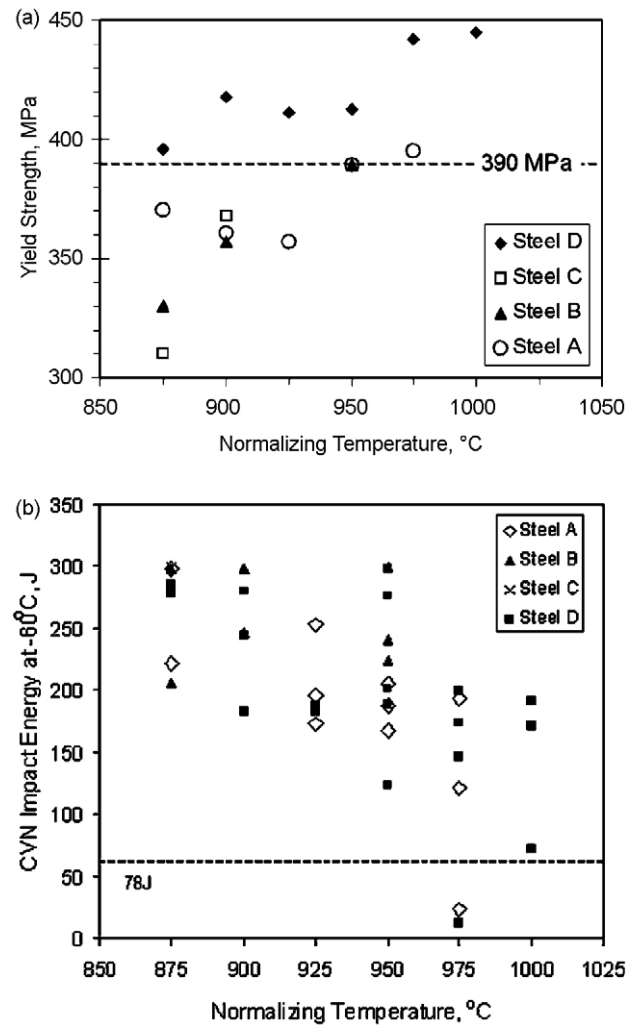


Fig. 2. Effect of normalizing temperature on (a) yield strength, and (b) CVN impact energy at -60°C for steels A–D.

- (b) The loss of yield strength upon normalizing, expressed as percentage *softening* relative to the as-rolled yield strength, is shown in Fig. 3. At 875°C normalizing, both steels B and C show a softening of $\sim 30\%$ while steels A and D both exhibit softening

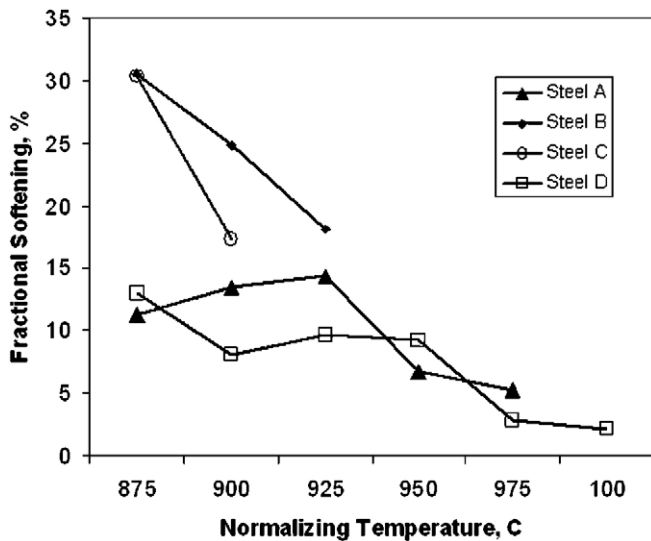


Fig. 3. Loss of yield strength upon normalizing, expressed as percentage softening relative to the as-rolled yield strength.

of $\sim 12\%$ only. However, it must be noted that even this small extent of softening in steel A is sufficient to reduce the yield strength below specification. For normalizing between 900 and 950 °C, steel D exhibits the lowest softening amongst the different samples tested, with YS that is nearly 90% of that in as-rolled condition. In contrast, steel B shows the maximum softening for the three normalizing temperatures (875, 900 and 925 °C) for which its properties were determined.

Fractographs of CVN impact tested samples of steel D in the as-rolled and 925 °C normalized condition show cleavage and ductile modes of fracture respectively. The cleavage fracture is responsible for the extremely low impact energy (5J) in the as-rolled condition. On the other hand, in the normalized sample, the processes of nucleation, growth and coalescence of voids has resulted in much higher energy absorption (184J) in the process of fracture. This behaviour is representative of all the four steels considered in the present study.

As steels B and D have similar levels of vanadium with the latter having no titanium, a thorough comparative evaluation of the microstructures of these two steels, in the as-rolled and the normalized (at 900 °C) conditions, has been performed using optical, scanning and transmission electron microscopy.

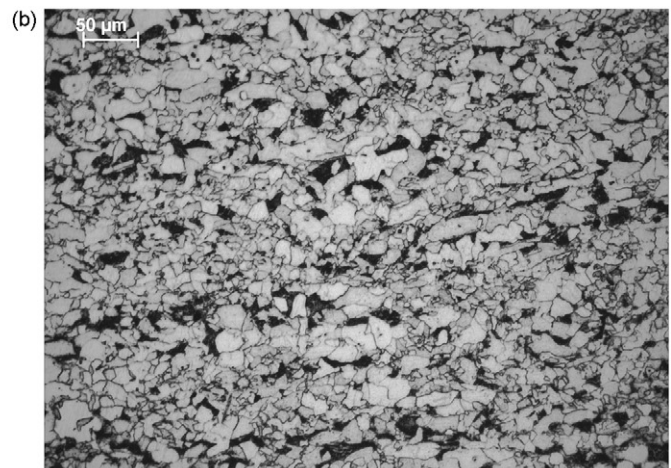
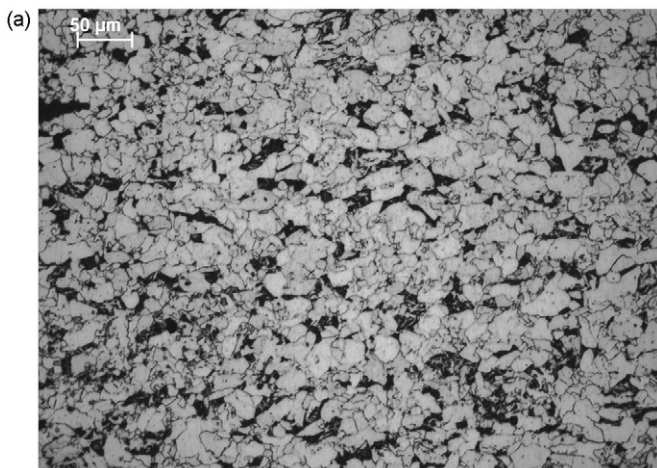


Fig. 4. Optical micrographs for (a) steel B and (b) steel D in the as-rolled condition.

3.2. Optical metallography

Typical optical micrographs of the as-rolled plates of steels B and D (Fig. 4) reveal that the microstructure consists of predominantly polygonal ferrite and small amounts of a dark etching second phase. The latter, wherever resolvable, could be identified as pearlite. Similar microstructure was observed in steels A and C also.

Banded regions of relatively coarser and finer ferrite grains suggesting a bimodal grain size distribution is observed. This corresponds to Type III of topologically varying duplex structure as described in ASTM E1181. To further quantify the extent of bimodality, the approach suggested by Chakrabarti et al. [19] using area-weighted histograms has been employed, as it has been reported that this approach is superior to using number-frequency histograms in revealing bimodality [19,20]. Area percent histograms (Fig. 5) as a function of equivalent circle diameter (ECD) were generated for both steel microstructures using at least 1500 grains seen in Fig. 4. ECD is the diameter of a circle that has the same area as the grain. ECD values range from less than 2 μm to more than 35 μm . The bimodal nature of the distribution is clearly evident, especially for steel B, with two peaks occurring at ECD of 17.5 and 32.5 μm ; in the case of steel D, the respective peaks are at 12.5 and 22.5 μm . The small separation (peak grain size range, PGSR, as defined in Ref. [19]) of 10 μm between the two peaks in the latter case implies a considerable overlap in the two distributions, in contrast to the 15 μm separation seen in the case of steel B. In the nomenclature introduced by Chakrabarti et al. [19], steels B and D have bimodality levels of 3 (quite bimodal) and 2 (average bimodal) respectively. This analysis results in an average grain size of 8.82 ± 5.59 and 7.36 ± 4.76 μm for steels B and D respectively. Using the lineal intercept method as per ASTM E-112, the average grain size was found to be 10.7 and 10.5 μm for steels B and D respectively. This shows that the ASTM method tends to slightly over-estimate the average grain size; however, it is much quicker and more convenient than the detailed analyses involving areas of individual grains.

The normalizing treatment results in a more homogenous microstructure, as shown for steel D (Fig. 6). Using the lineal intercept method, the average grain size in the normalized condition was found to be 6.7 and 7.4 μm for steels B and D respectively, relative to ~ 10.5 μm in the as-rolled structure.

3.3. Scanning electron microscopy

Secondary electron micrographs of the as-rolled and the normalized plates of steels B and D are shown in Fig. 7. The refinement

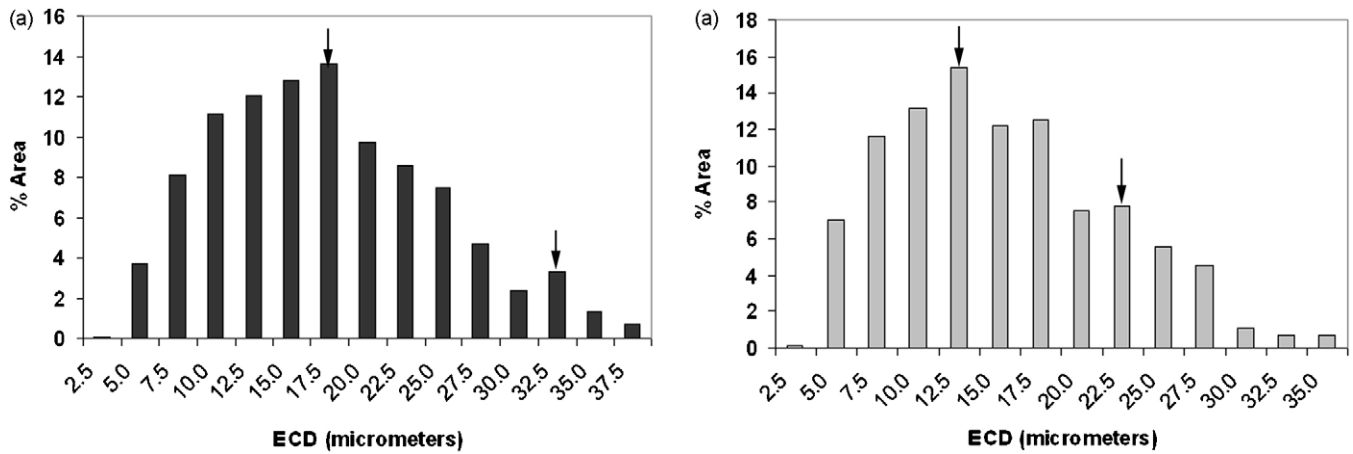


Fig. 5. Area percent grain size distributions measured from optical micrographs as function of equivalent circle diameter (ECD) for (a) steel B and (b) steel D in the as-rolled condition. The two peaks are indicated with arrows.

of grain size upon normalizing is clearly evident. For the normalized samples, a detailed analysis of the grain size distributions (GSDs) has been carried out using the secondary electron images shown in Fig. 7b and d, as the grain boundaries were more clearly delineated in these images than in the optical micrographs. Area percent histograms of the normalized samples (Fig. 8) were generated using at least 350 ferrite grains from each sample. The first and second peaks in the GSD for steel B (D) occur at $9\ \mu\text{m}$ ($9\ \mu\text{m}$) and $16.5\ \mu\text{m}$ ($19.5\ \mu\text{m}$) respectively. Further, the area fraction occupied by larger grains has significantly reduced. In the case of steel B, this is also reflected in a large downward shift of the second peak from $32.5\ \mu\text{m}$ in the as-rolled condition to $16.5\ \mu\text{m}$ in the normalized condition. The average grain size obtained from this analysis is found to be $\sim 6\ \mu\text{m}$ in both cases. These observations provide a quantitative confirmation of the microstructural refinement upon normalizing.

Detailed examination of the second phase shows that it is classical lamellar pearlite in some cases, but more often, it exhibits a discontinuous morphology. Based on the chemical composition of the steel and its thermal history, this phase is likely to be degenerate pearlite [21]. The etched samples also revealed the presence of inclusions that were, at times, several tens of μm in length. Detailed study revealed that the inclusions were similar (in terms of morphology, extent, amount etc.) in both steels except for one major difference: in the case of steel B, aggregates of inclusions rich in Ti and N (Fig. 9a and b) were seen in association with faceted Al

and O rich inclusions (Fig. 9c). No such inclusions were seen in steel D.

3.4. Transmission electron microscopy

Representative TEM micrographs obtained from steels B and D in the as-rolled condition are given in Fig. 10. The striking difference between the two steels is the absence of fine precipitates in steel B. Given the likely heterogeneous nature of the distribution of these precipitates, several ferrite grains from different regions of the sample were carefully analysed, but not many sub-100 nm precipitates could be observed in this steel. A few inclusions of size $0.5\text{--}1\ \mu\text{m}$ were observed, which were shown by EDS to be manganese sulfides.

In steel D, precipitates with size from 2 to 20 nm were observed (Fig. 10b). Size measurements on more than 200 such precipitates yielded an average size of $6.55 \pm 3\ \text{nm}$ (Fig. 11) in the as-rolled sample. It must be noted that the spatial distribution of these precipitates is rather heterogeneous. There are several grains that contain no precipitates and even within grains that do contain them, there are regions that are precipitate-free. Similar reports exist in the literature [13,22,23] regarding the heterogeneous distribution of fine precipitates. These reports attribute this heterogeneity to the segregation of alloying elements to the inter-dendritic regions during solidification. While random heterogeneously distributed precipitates were most frequently observed, occasionally, aligned rows of particles as well as those nucleated preferentially on dislocations were also seen (Fig. 12a and b). The fine size of the particles makes it difficult to determine their composition by EDS. But, the steel composition and the thermal history suggest that these particles are likely to be vanadium carbonitrides [13].

For both steels B and D, the microstructure of the normalized sample was essentially similar to the corresponding as-rolled samples. The particle size distribution (Fig. 11) shows an increased fraction of coarser particles for the normalized steel D sample relative to the as-rolled sample, with an average size of $7.21 \pm 3.68\ \text{nm}$.

4. Discussion

Several strengthening mechanisms such as solid solution, grain size, dislocation, precipitation etc., will contribute to the yield strength of HSLA microalloyed steels [24]. An additive effect of the different strengthening mechanisms is commonly assumed and several empirical equations exist [22,25–29] to estimate the relative contributions of the different strengthening mechanisms to the

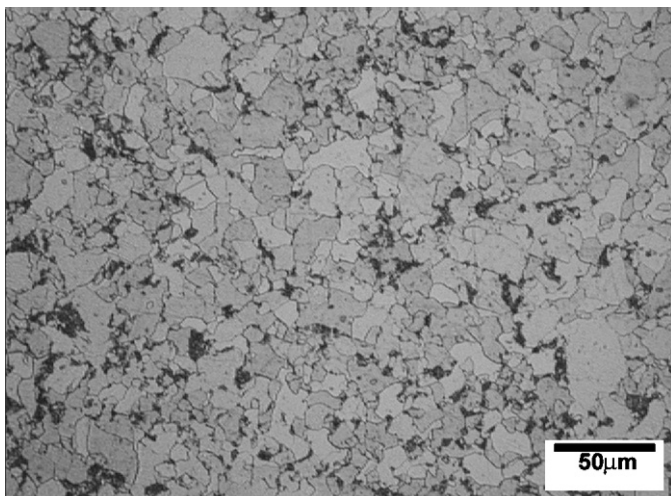


Fig. 6. Optical micrograph for steel D normalized at $900\ ^\circ\text{C}$.

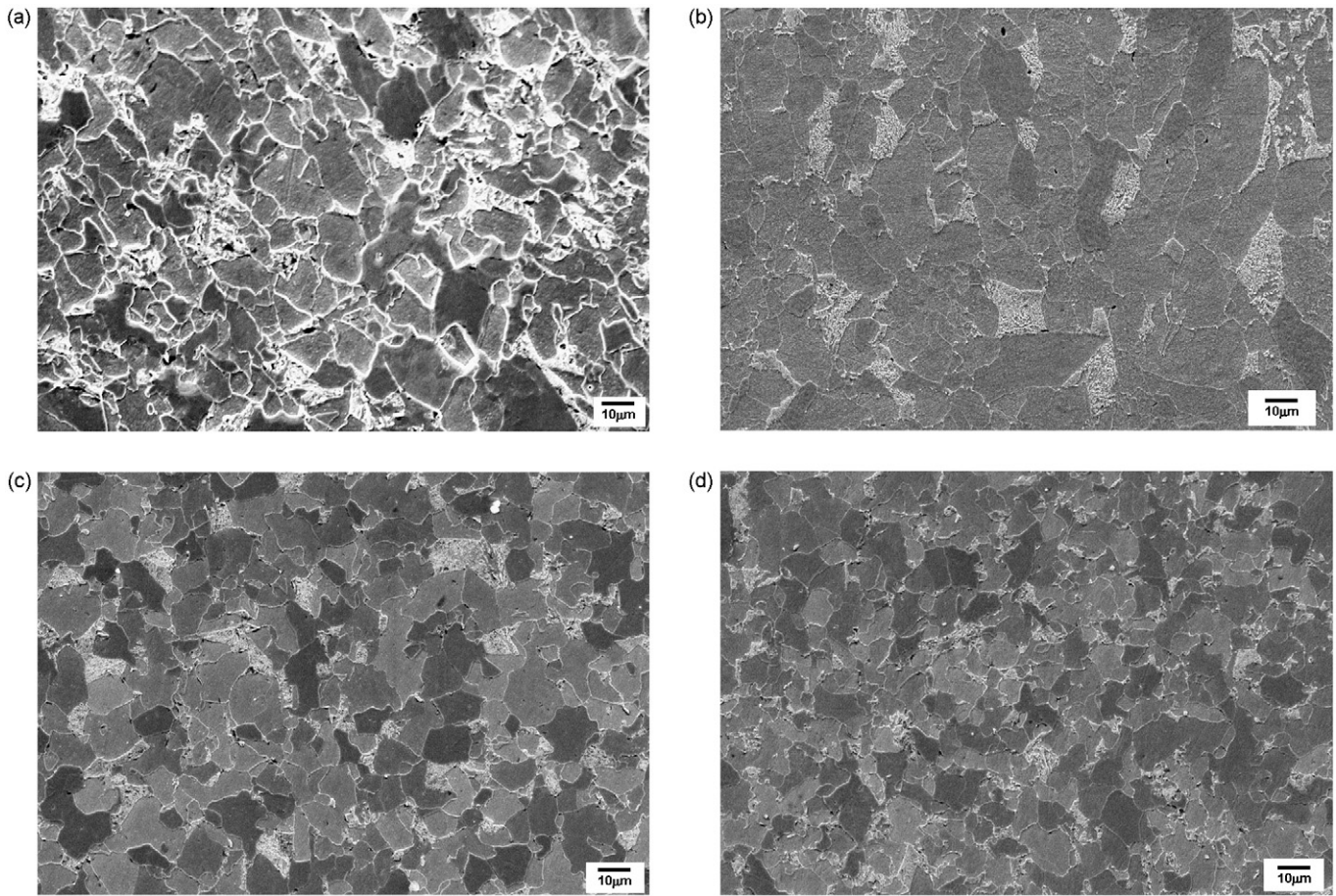


Fig. 7. SEM micrographs: (a) steel B, as-rolled, (b) steel D, as-rolled, (c) steel B, normalized at 900 °C, and (d) steel D, normalized at 900 °C.

yield strength. Kestenbach et al. [26] have found the equation due to Pickering [30] to be most suited for microalloyed steels such as the ones being considered in the present work:

$$\sigma_y [\text{MPa}] = 15.4(3.5 + 2.1 \text{ pct Mn} + 5.4 \text{ pct Si} + 23 \text{ pct N}_f + 1.13 d^{-1/2})$$

where pct Mn, pct Si, pct N_f are the weight percentages of manganese, silicon, and free nitrogen respectively, dissolved in ferrite, and d is the ferrite grain size in mm. The above equation considers only solid solution and grain size strengthening. The difference

between the experimental and calculated yield strength values can be considered to be the contribution from *other strengthening mechanisms* including precipitation hardening.

In the present work, free nitrogen has been assumed to be negligible because of the presence of strong carbide/carbonitride forming elements in sufficient amounts. The different contributions to the yield strength of steels B and D in the as-rolled and the normalized conditions calculated using the above equation is shown in Fig. 13. The lattice and solid solution strengthening con-

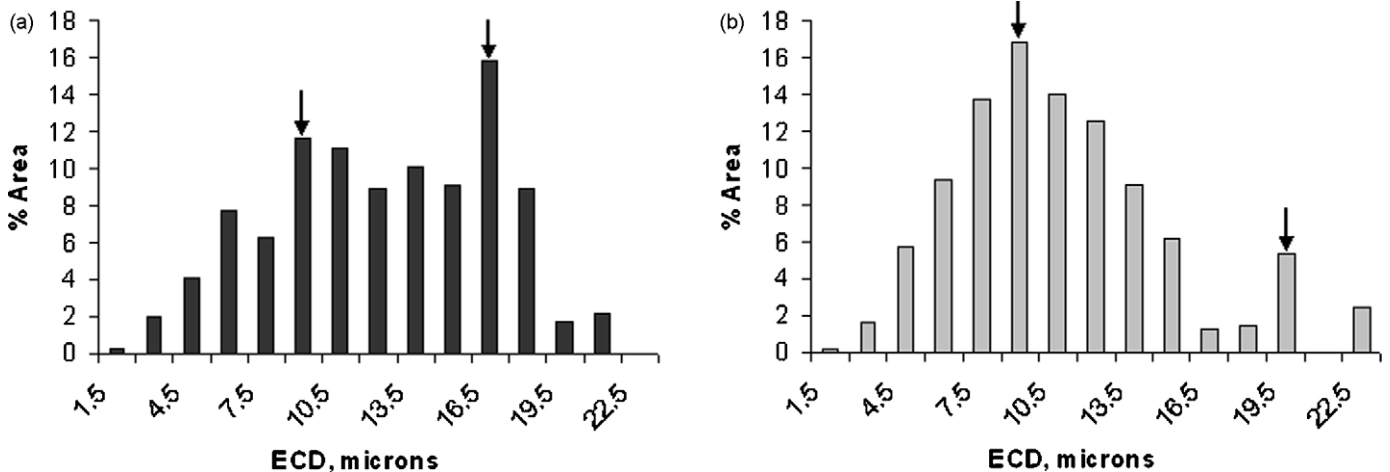


Fig. 8. Area percent grain size distributions measured from SEM micrographs as function of equivalent circle diameter (ECD) for (a) steel B and (b) steel D, normalized at 900 °C. The two peaks are indicated with arrows.

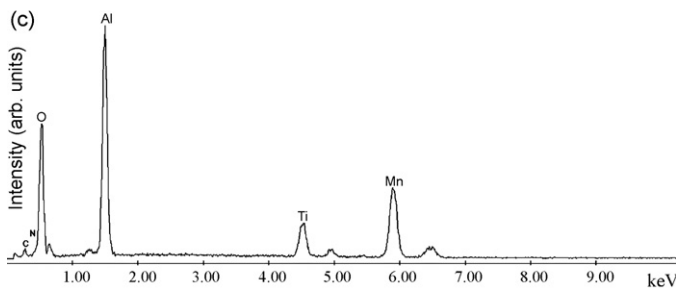
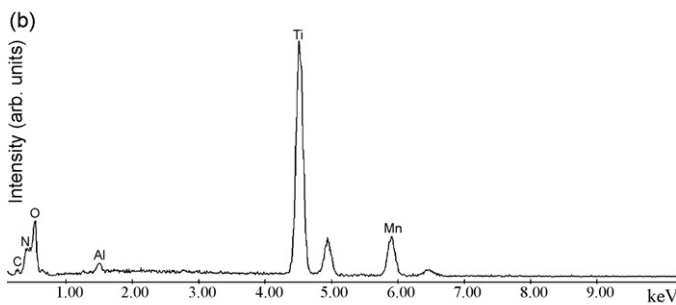
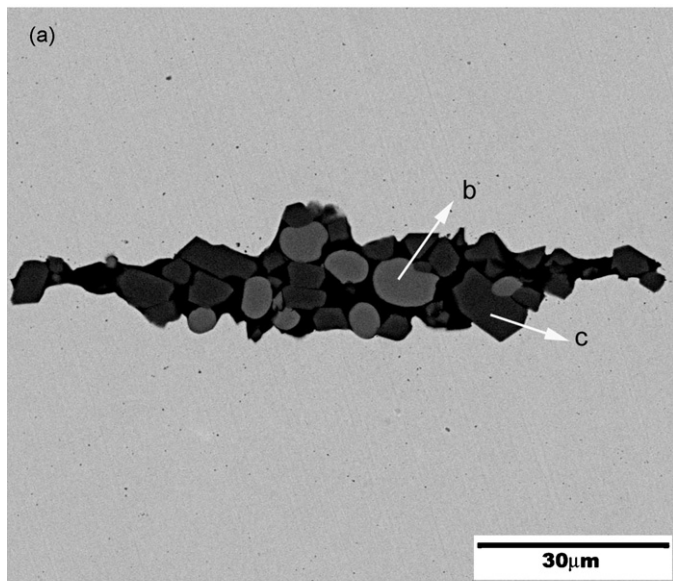


Fig. 9. (a) SEM micrograph showing the aggregate of inclusions in steel B in the as-rolled condition, (b) and (c) are the EDS spectra respectively for the Ti rich and Al rich inclusions indicated in (a).

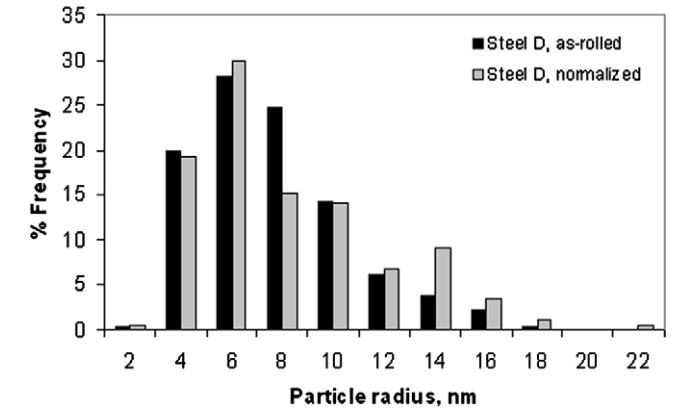
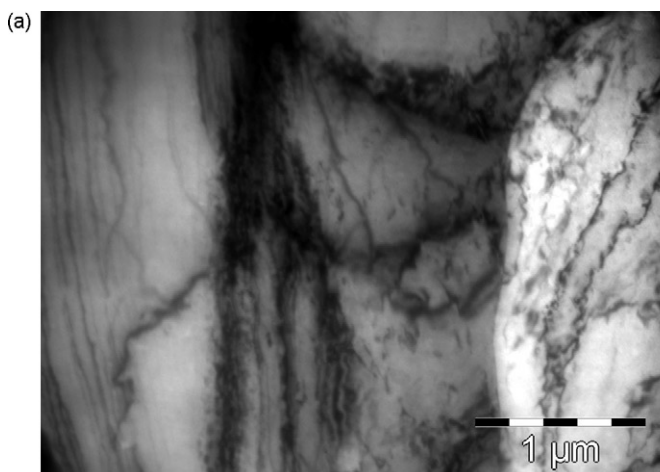


Fig. 11. Particle size distribution for steel D in the as-rolled and normalized conditions obtained from TEM micrographs.

tributions are similar in both steels; also, they remain unaffected by the normalizing treatment. However, the contribution due to grain size has increased in both steels (by 45 MPa in steel B and 32 MPa in steel D) as a result of the grain refinement. For these calculations, the average grain size as calculated by the lineal intercept method (section 3.2) has been employed. More interestingly, the contribution due to other mechanisms has dramatically dropped in steel B (by nearly 87%), from 187 MPa in the as-rolled condition to 24 MPa in the normalized condition. In contrast, the decrease in steel D is significantly less (only by 41%), from 168 to 99 MPa. Consequently, steel D is still able to meet the specified yield strength after normalizing whereas the normalized steel B plate falls short by ~ 30 MPa. Based on SEM and TEM microstructural observations, it can be inferred that while there is significant amount of precipitation strengthening in steel D in both as-rolled and normalized conditions, no such contribution exists for steel B in either condition. Clearly, the ‘additional strengthening’ in steel B, in both as-rolled and normalized conditions, is due to mechanisms other than precipitation strengthening.

The most striking feature of the steel B microstructure is the absence of the fine (sub-100 nm) precipitates. As mentioned earlier, the steel contains several large inclusions of TiN. This implies that adequate nitrogen is not available in solution for the formation of fine precipitates during subsequent stages. In contrast, the absence of Ti in steel D implies that nitrogen is not locked up as TiN thereby enabling the precipitation of fine carbonitride particles, which contribute to precipitation strengthening. Further support for this has been obtained from thermodynamic calculations for steels B and D

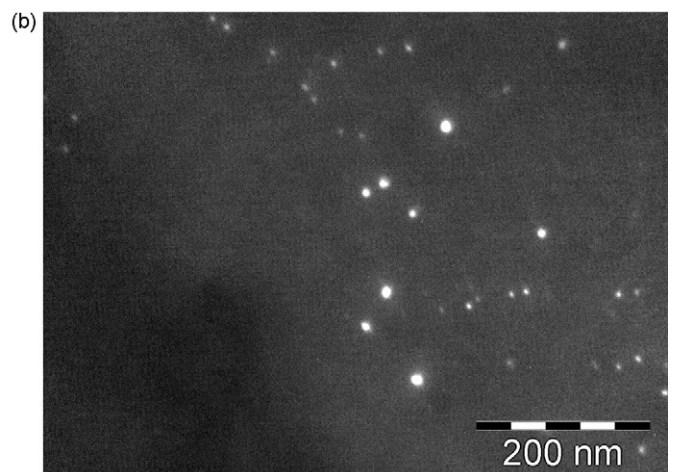


Fig. 10. TEM micrographs in the as-rolled condition: (a) bright field image showing the absence of fine precipitates for steel B, and (b) dark field image showing the presence of fine precipitates for steel D.

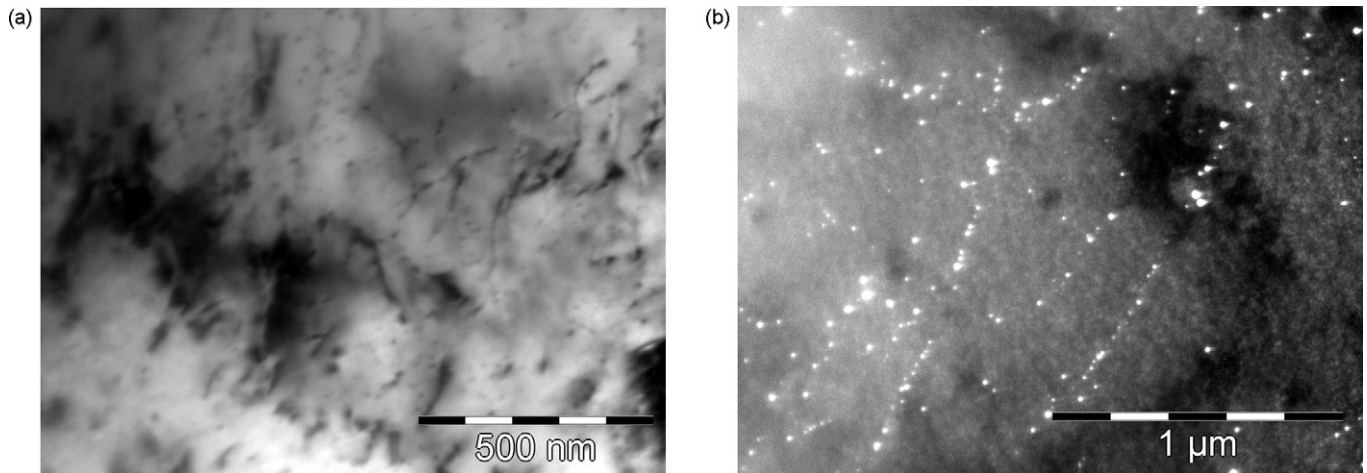


Fig. 12. TEM micrographs for steel D in as-rolled condition: (a) bright field image showing the presence of fine precipitates on dislocations, and (b) dark field image showing the interphase and random distribution of precipitates.

performed using ThermoCalc software [31]. The calculations predict an A_3 temperature of $\sim 830^\circ\text{C}$ (in both steels), which is about 30°C less than the experimentally reported Ar_3 value. Nevertheless, the general trends as predicted by the simulations can be used to rationalize the experimental observations.

Figs. 14 and 15 show the equilibrium molar volume fractions and the composition of the MX ($M=\text{Ti, Nb, V}$; $X=\text{C, N}$) carbonitride phase respectively in the two steels. In steel B, precipitates of the MX phase start forming during the early stages of solidification at temperatures in the vicinity of 1500°C , even prior to the formation of austenite, and continue to grow as the temperature falls and solidification proceeds. Therefore these precipitates are likely to be coarse (order of a few μm). Once present in the slab, these coarse precipitates are unlikely to dissolve during any subsequent processing that involves temperatures of the order of 1250°C (for soaking prior to rolling) or lower. At very high temperatures, the phase is essentially TiN, but increasing amounts of vanadium and niobium, in approximately equal extent, are incorporated into the phase with decreasing temperature (Fig. 15a) – at $\sim 1200^\circ\text{C}$, the metal sublattice contains (in at.%) 62 Ti, 20 V and 18

Nb. Therefore, the presence of even a few of these precipitates drastically reduces the available amounts of nitrogen and vanadium in solution (in austenite) required for the formation of fine carbonitride precipitates either during rolling or normalizing. Clearly, these large particles correspond to the titanium-rich inclusions observed in the SEM. One large particle of $1\text{-}\mu\text{m}$ diameter is equivalent (in volume) to 10^6 particles of 10 nm diameter. This may be the primary reason why only few fine precipitates are observed in steel B, either in the as-rolled or in the normalized condition.

The increase in the amount of MX phase between 1200 and 1000°C (Fig. 14) could be by accretion to the existing coarse particles as well as by nucleation and growth of new particles in the austenite. In the $1000\text{--}800^\circ\text{C}$ range, the molar fraction of the MX remains more or less constant. However, as the temperature falls below A_3 ($\sim 800^\circ\text{C}$) and ferrite begins to form, there is a sharp increase in the amount of MX phase from 0.13% at 800°C to 0.22% at 660°C because of the precipitation that takes place due to the much reduced solubility of the microalloying elements in the evolving ferrite matrix. However, the presence of only a few precipitates in steel B indicates that the precipitation at lower temperatures must have taken place heterogeneously on the larger nitride/oxide inclusions. Indeed, evidence for this can be seen from back-scattered

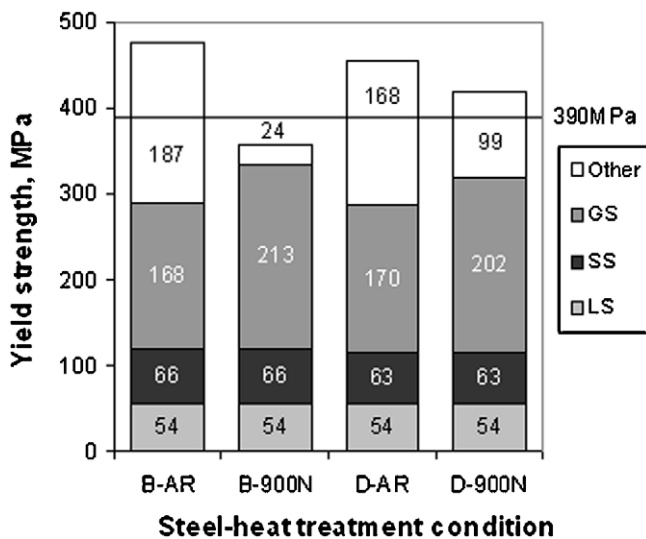


Fig. 13. Contributions from different strengthening mechanisms for steels B and D in as-rolled and normalized conditions – lattice strengthening (LS), grain size (GS) strengthening, and solid solution (SS) strengthening; ‘other’ includes mechanisms such as dislocations, fine precipitates etc.

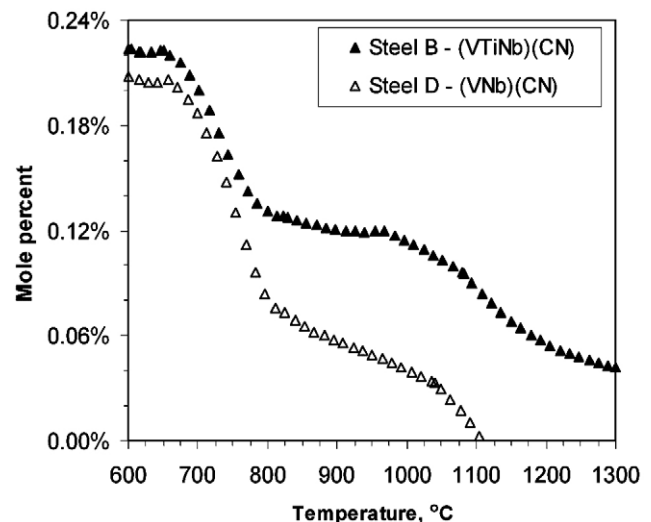


Fig. 14. Amount (in mol.%) of MX phase in steels B and D as a function of temperature.

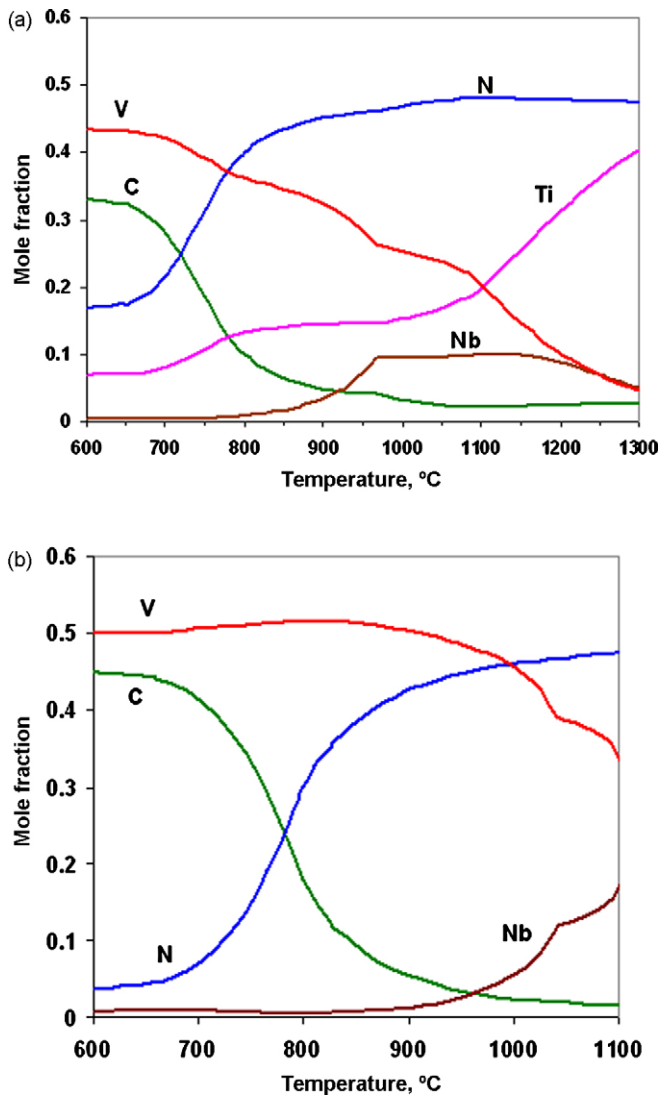


Fig. 15. Composition of MX phase as function of temperature in (a) steel B and (b) steel D.

electron images (Fig. 16), where the brighter contrast of the small particles suggests enrichment of Nb and/or V.

In steel D, the MX phase is present only at temperatures lower than 1110 °C, which is well below the usual soaking temperature (~1200–1250 °C) prior to hot-rolling. In this steel, upon normalizing, significant amount of the MX phase goes into solution (for $T > 900$ °C, less than 25% of the MX phase that was present at 660 °C remains undissolved), which is re-precipitated upon cooling from the austenitizing temperature. In the normalizing regime, the remnant MX phase is predominantly vanadium nitride, but during cooling, the newer precipitates to form are mostly carbides. A key difference between the two steels is the difference in the composition of the MX phase at lower ($T < 650$ °C) temperatures (Fig. 15). The equilibrium composition in steel B accommodates much more nitrogen than that in steel D.

One possible concern might arise regarding the differences between laboratory scale and industrial scale processing, especially regarding the role of titanium. In the present study, the steel was homogenized at 1225 °C for 24 h before forging, and the slab was soaked at 1180 °C for 3 h prior to rolling. In contrast, the soaking temperatures in the industry tend to be much higher (>1250 °C); often, the soaking times are also longer. In order to prevent excessive grain growth under these conditions, a small

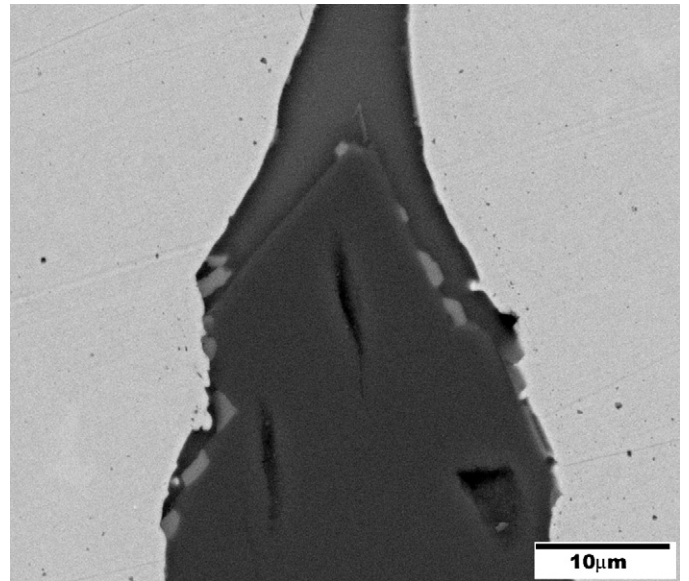


Fig. 16. BSE micrograph showing small particles (bright) nucleated at the edges of oxide inclusions in aggregates.

amount of titanium (say, 0.002–0.004 wt.%) is essential because, at these high temperatures, only titanium nitride particles remain; all other MX ($X = C, N$) particles including niobium carbonitrides go into solution. For similar reasons, titanium is also required to prevent excessive grain growth in the heat affected zone (HAZ) during welding of plates [3]. Thus, while the present study suggests that titanium may not be needed in the case of normalized steels, a small amount of titanium should nevertheless be incorporated in order to prevent excessive grain growth at high temperatures seen during soaking prior to rolling and also, in the HAZ, during welding. Of course, with the addition of this low level of titanium to the steel, some amount of vanadium and nitrogen would be incorporated into the TiN particles. Therefore, the levels of these elements in the steel would have to be enhanced marginally to ensure adequate V(C, N) precipitation similar to that in steel D. The additional requirements of vanadium and nitrogen can be determined by further calculations using ThermoCalc.

5. Summary and conclusions

DMR-249A plates that are currently used meet specified properties in the as-rolled condition for thickness up to 16 mm, but thicker plates require a water quenching and tempering treatment to meet property specifications. Present study was carried out to address the need for steels of heavier gage (thickness 18–40 mm) that could meet properties in the as-rolled or normalized condition, without the need for a water quenching and tempering treatment. This was attempted through the improvisation of composition of the DMR-249A steel. Specifically, 24 mm thick hot-rolled plates of experimental steels with ~0.015 wt.% Ti at three enhanced vanadium levels (0.06, 0.09 and 0.12 wt.%) were investigated. In addition, one steel with 0.10 wt.% V and no Ti was also studied.

1. In the as-rolled condition, the steels A–D meet yield strength specification but exhibit poor impact toughness. In the normalized condition, only steel D consistently meets both YS and CVN properties while other steels fall short of YS specification.
2. Microstructural characterization of steels B and D reveals two major differences:
 - a. the presence of large Ti and nitrogen rich inclusions in steel B, which are absent in steel D; and

- b. the near complete absence of fine (sub-100 nm) precipitates in steel B.
- In steel B, the large Ti and N rich inclusions are likely to have depleted the matrix of Nb and V thereby resulting in a significant reduction in the number of fine strengthening precipitates dispersed in the matrix. This is believed to be the main reason for the inability of steel B to meet yield strength requirements in the normalized condition.
 - In contrast, in steel D (which has no Ti), only oxide inclusions are seen in the microstructure implying that sufficient nitrogen (as well as Nb and V) is in solution in the austenite matrix and is available for subsequent precipitation of fine particles of nitrides (or carbonitrides). The fine particles observed in steel D in as-rolled condition are between 2 and 20 nm in size. Based on steel composition, thermal history and thermodynamic calculations, these are likely to be V-rich carbonitrides. Upon normalizing, these V-rich particles dissolve and re-precipitate upon cooling without significant change in the particle size distribution. Thus, the significant contribution from precipitation strengthening ensures that steel D meets the yield strength requirement in the normalized condition.
 - Finally, a plateau in yield strength, seen in the case of steel D samples normalized in the 900–950 °C range, taken in conjunction with the fact that these samples exhibit sub-zero impact toughness in excess of 180 J (average) has industrial significance as this allows a large temperature window for the normalizing treatment of large size heavy gage plates.

Acknowledgements

This research was funded by the Defence Research and Development Organization (DRDO), India, under Project DMR-249. The authors thank Dr. D. Banerjee, Chief Controller R&D (AMS), DRDO for his keen interest, constant encouragement and guidance throughout the project. The authors wish to thank Dr. K. Muraleedharan and Dr. M. Srinivas, Defence Metallurgical Research Laboratory, Hyderabad and Prof. K.K. Ray, IIT Kharagpur for useful discussions. The authors are also thankful to different groups of DMRL for their assistance in plate rolling, mechanical testing, heat treatment and metallography. The authors wish to thank the reviewer for many useful comments and suggestions.

References

- A.C. Kneissl, C.I. Garcia, A.J. DeArdo, in: G. Tither, Z. Shouhua (Eds.), HSLA Steels, Processing, Properties and Applications, The Minerals, Metals & Materials Society, 1992, pp. 99–105.

- P.C.M. Rodrigues, E.V. Pereloma, D.B. Santos, Mater. Sci. Eng. A 283 (2000) 136–143.
- L. Meyer, C. Straßburger, C. Schneider, Proc. Int. Conf. on HSLA Steels: Metallurgy and Applications, Beijing, People's Republic of China, 4–8 November, 1985, pp. 29–44.
- B.K. Show, Effect of V and Cu on the structure and properties of microalloyed HSLA steel, M. Tech thesis, Indian Institute of Technology, Kharagpur, India, 2007.
- J. Kong, C. Xie, Mater. Des. 27 (2006) 1169–1173.
- N. Venkateswara Rao, B.S. Bansal, K. Ankalu, A. Dutta, M. Srinivas, K. Muraleedharan, R. Balamuralikrishnan, G. Malakondaiah, Met. Mater. Proc. 19 (2007) 261–272.
- T. Gladman, The Physical Metallurgy of Microalloyed Steels, The Institute of Material, London, 1997, pp. 280–288.
- E.E. Fletcher, High Strength Low Alloy Steels: Status, Selection and Physical Metallurgy, Battelle Press, Columbus, OH, 1979, p. 135.
- E.E. Fletcher, High Strength Low Alloy Steels: Status, Selection and Physical Metallurgy, Battelle Press, Columbus, OH, 1979, pp. 137–139.
- T. Gladman, The Physical Metallurgy of Microalloyed Steels, The Institute of Material, London, 1997, p. 187.
- J.J. Jonas, Mater. Sci. Eng. A 184 (1994) 155–165.
- Y. Li, D.N. Crowther, P.S. Mitchell, T.N. Baker, ISIJ Int. 42 (2002) 636–644.
- S. Zajac, T. Siwecki, W.B. Hutchinson, R. Lagneborg, ISIJ Int. 38 (1998) 1130–1139.
- B.K. Show, B. Rajendra Prasad, G. Balachandran, Air Induction Melting of DMR249A Naval Steels at AV Alloys Ltd., DMRL TR430, DMRL, Hyderabad, India, 2007, pp. 1–22.
- K. Muraleedharan, A. Verma, R. Balamuralikrishnan, unpublished research (2005).
- ASTM E 8M-03: Standard Test Methods For Tension Testing of Metallic Materials [Metric], 2004.
- ASTM E 23-02a: Standard Test Methods for Notched Bar Impact Testing of Metallic Materials, 2004.
- UTHSCSA, Image Tool for windows, Ver. 3.00, University of Texas Health Science Center in San Antonio.
- D. Chakrabarti, C. Davis, M. Strangwood, Mater. Charact. 58 (2007) 423–438.
- G.F. Van der Voort, J.J. Friel, Mater. Charact. 29 (1992) 293–312.
- S. Shanmugam, R.D.K. Misra, T. Mannering, D. Panda, S.G. Jansto, Mater. Sci. Eng. A 437 (2006) 436–445.
- Y. Li, J.A. Wilson, A.J. Craven, P.S. Mitchell, D.N. Crowther, T.N. Baker, Mater. Sci. Technol. 23 (2007) 509–518.
- H. Najafi, J. Rassizadehghani, A. Halvaeae, Mater. Sci. Technol. 23 (2007) 699–705.
- R.D.K. Misra, G.C. Weatherly, J.E. Hartmann, A.J. Boucek, Mater. Sci. Technol. 17 (2001) 1119–1129.
- T. Gladman, The Physical Metallurgy of Microalloyed Steels, The Institute of Material, London, 1997, pp. 19–57.
- H.-J. Kestenbach, S.S. Campos, E.V. Morales, Mater. Sci. Technol. 22 (2006) 615–626.
- R.D.K. Misra, H. Nathani, J.E. Hartmann, F. Siciliano, Mater. Sci. Eng. A 394 (2005) 339–352.
- J. Cao, Q. Yong, Q. Liu, X. Sun, J. Mat. Sci. 42 (2007) 10080–10084.
- R.J. Glodowski, 42ND MWSP Conf. Proc. ISS XXXVIII (2000) 441–451.
- F.B. Pickering, Physical Metallurgy and the Design of Steel, Applied Sci. Publ., London, 1978, p. 63.
- Thermo-Calc for Windows, Ver. 4, <http://www.thermocalc.se/>: with TCFE5 database, Stockholm, Sweden.